Negative magnetoresistance of pyrolytic carbon and effects of low-temperature electron irradiation

A. Iwase, N. Ishikawa, T. Iwata, and Y. Chimi
Department of Materials Science, Japan Atomic Energy Research Institute, Tokai-mura, Naka-gun, Ibaraki, 319-1195, Japan

T. Nihira
Faculty of Engineering, Ibaraki University, Hitachi, Ibaraki, 316-8511, Japan
(Received 12 April 1999; revised manuscript received 17 June 1999)

Pyrolytic carbon that exhibits negative magnetoresistance is irradiated with 2 MeV electrons at temperatures below 35 K, and the changes in electronic transport properties such as zero-magnetic field resistivity, Hall coefficient, and magnetoresistance are measured as a function of electron fluence. With increasing electron fluence, the zero-field resistivity decreases, while the Hall coefficient and the absolute values of negative magnetoresistance increase. The experimental data are analyzed assuming that the densities of electrons and holes vary with the magnetic field. The analysis shows that the densities increase with the square of the magnetic field; the result is in good agreement with the Bright theory, in which the two-dimensional Landau levels are assumed to be broadened due to defect scattering. Both intrinsic defects and irradiation-produced defects act as electron acceptors. The addition of acceptors increases the ratio of hole density to electron density, p/n, resulting in the enhancement of negative magnetoresistance. The present results clarify that the negative magnetoresistance in pyrolytic carbon is caused by the existence of acceptor defects and the two-dimensional Landau levels, which are broadened by the defects. In addition, they suggest that the intrinsic acceptor defects in pyrolytic carbon are presumably vacancies. [S0163-1829(99)05439-9]

I. INTRODUCTION

It is well known that poorly graphitized carbons exhibit peculiar behaviors of electronic transport properties, such as negative magnetoresistance, Hall coefficients inversely proportional to the applied magnetic field at low temperatures and so on. First, Mrozowski and Chaberski discovered that in disordered pregraphitic carbons the electrical resistivity decreased with increasing the magnetic fields.[1] Since then, this unusual phenomenon has been found also in a lot of pregraphitized carbon materials.[2–13]

One of the characteristics of poorly graphitized carbons is their turbostratic structure, i.e., random stacking of graphene layer planes.[14,15] This structure causes a larger *c*-axis lattice parameter and then a more two-dimensional (2D) electron system than those of highly graphitized samples. By using Wallace's 2D band structure for graphite,[16] McClure obtained the energy levels (Landau levels) of 2D free-electron system for graphite under the magnetic field and showed that the state density of each level was proportional to the magnetic field.[17] Uemura and Inoue analyzed the result of Hall coefficient for graphite by considering the change in carrier concentration with the magnetic field, which was induced by the formation of the 2D Landau level, and assuming a discrete acceptor level in the π band.[18] Further, Yazawa added a constant state density at the $n=0$ Landau level as a result of 3D correlations between layer planes, and explained the negative magnetoresistance and the magnetic-field dependence of the Hall coefficients of pyrolytic carbon.[4,19] Afterward, Bright refined Yazawa's analysis by adding the effect of defect- and phonon-induced broadening of the Landau level.[20] His theory could quantitatively reproduce the experimental result of negative magnetoresistance for several carbon fibers heat treated at the different temperatures. Then, it predicts that the density of states increases with the square of the applied magnetic field at lower fields.

In 80s, a completely different mechanism was applied for the explanation of negative magnetoresistance in poorly graphitized carbons. To explain the galvanomagnetic behavior of grafoil, Koike *et al.*[10] applied the theory of Abrahams, Anderson, Licciardello, and Ramakrishnan[21] for the first time, and later Piraux *et al.*[22,23] and Bayot *et al.*[12,13] analyzed the data of negative magnetoresistance in intercalated graphite fibers, pyrocarbon and so on within the frame work of this theory. The theory of Abrahams *et al.* predicts that, in the disordered 2D electron system, interference effects induce the weak localization of propagating electrons.[24] Under the magnetic field, the phase coherence between electron waves is destroyed and then the weak localization is suppressed. Therefore, the weak-localization theory explains the negative magnetoresistance as due to the increase in carrier mobility under the magnetic field.

No matter which mechanism is truly responsible for the negative magnetoresistance, there seems to be no doubt that the two dimensionality of electron system and the structural disorder (or lattice defects) play an important role in the appearance of negative magnetoresistance in poorly graphitized materials. We are interested in the type of intrinsic defects actively involved in the phenomenon. We assume that the first candidate of these defects is vacancies in graphitic layer planes and the most effective may be single vacancies, which are formed during pyrolytic deposition process.

We have artificially produced single vacancies in pyrolytic carbon by using 2 MeV electron irradiation at <35 K, where the interstitial atoms produced are considered to be

 ©1999 The American Physical Society

not so active, as discussed later. The density of vacancies produced can be controlled so as to change the carrier density considerably with hardly changing the carrier mobility.

We have measured the Hall coefficient and magnetoresistance as a function of magnetic field before and after the electron irradiations and after the thermal annealing. We have found that the electron irradiation accelerates the appearance of negative magnetoresistance. A theoretical consideration shows that the relation $p-n=N_\nu$ is valid independent of the temperature and magnetic field, where p, n, and N_ν are the density of holes, electrons and electron acceptors, respectively. Using this relation and the simple two-band model, we have calculated the carrier densities as functions of magnetic field and electron fluence. Both before and after irradiation, the carrier densities increase with the square of the magnetic field, which is in good agreement with the Bright theory. Both intrinsic and irradiation-produced defects act as electron acceptors. The addition of acceptors by the electron irradiation increases the ratio of hole density to electron density, and contributes to the enhancement of the negative magnetoresistance.

The present results clearly show that the negative magnetoresistance in pyrolytic carbon is caused by the existence of acceptor defects and the two-dimensional Landau levels broadened by the defects. In addition, they suggest that the intrinsic acceptor defects in pyrolytic carbon might be vacancies.

In the weak-localization approach, it will be expected that static lattice defects produced by electron irradiation accelerate the weak-localization effect and would give rise to an electrical resistivity increase. In the present experiment, however, the electrical resistivity at the zero-magnetic field decreases by the irradiation. Hence, we do not try to analyze the data in the framework of the weak-localization theory.

II. EXPERIMENTAL PROCEDURE

Specimen material for the present study was pyrolytic carbon deposited at about 2200 °C in the atmosphere of methane gas. Any heat treatment was not performed after deposition. A bridge-shaped specimen for basal plane resistivity and Hall coefficient measurements was cut from the material. The thickness of specimen was 0.28 mm.

In the present experiment, we used the irradiation apparatus interfaced to a dynamitron-type accelerator at JAERI (Japan Atomic Energy Research Institute)-Takasaki. This apparatus has been designed to allow both the electron irradiation at low temperatures and the subsequent *in situ* measurements of the galvanomagnetic properties under the magnetic fields of 0–6 T.

Before irradiation, zero-magnetic-field resistivity was measured as a function of temperature between 15 and 300 K. The Hall coefficient and magnetoresistance were also measured at 30, 50, 100, 200, and 300 K applying the magnetic field of 0–6 T perpendicular to the basal plane.

Then, the specimen was irradiated with 2.0-MeV electrons to the fluence of $4.5\times10^{20}/\mathrm{m}^2$, $9.6\times10^{20}/\mathrm{m}^2$, $1.4\times10^{21}/\mathrm{m}^2$, and $1.9\times10^{21}/\mathrm{m}^2$. During the irradiation, the specimen temperature was kept below 35 K. After each irradiation, the zero-magnetic-field resistivity was measured as a function of temperature between 15 and 30 K, and the magnetoresistance and Hall coefficient were measured at 30 K as a function of magnetic field. Subsequently, to study the recovery of galvano-magnetic properties, the specimen was annealed up to 300 K. During the annealing process, the zero-magnetic-field resistivity was measured as a function of temperature. Hall coefficient and magnetoresistance were measured at 300 K after annealing, and at 30 K after cooling down the specimen temperature. Finally, the zero-field-resistivity was measured again as a function of temperature between 30 and 300 K.

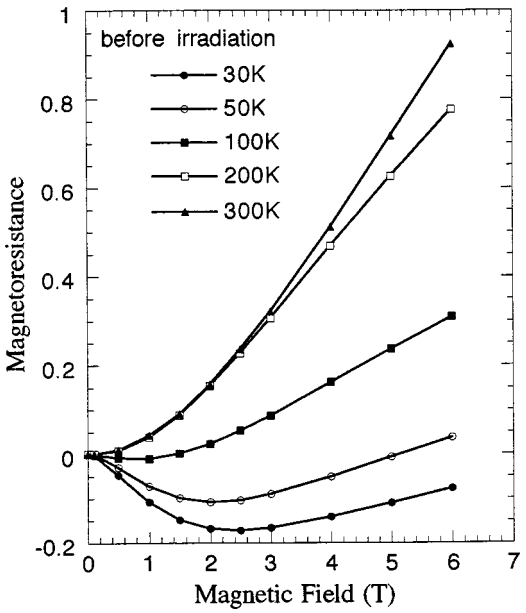

FIG. 1. Magnetic field dependence of magnetoresistance of unirradiated pyrolytic carbon at various temperatures.

III. EXPERIMENTAL RESULTS

In Fig. 1, the magnetoresistance for unirradiated specimen is plotted against the magnetic field taking the measurement temperature as a parameter. Magnetoresistance is defined as

$$\frac{\Delta\rho}{\rho_0}=\frac{\rho(H)-\rho_0}{\rho_0}, \tag{1}$$

where $\rho(H)$ is the resistivity under the magnetic field H, and ρ_0 is the zero-field resistivity.

Figure 2 shows the Hall coefficients of unirradiated specimen as a function of magnetic field with the measurement temperature as a parameter.

Figure 3 presents the effect of 2-MeV electron irradiation on the zero-field resistivity between 15 and ~30 K. Electron irradiation causes the decrease in basal plane resistivity. Negative temperature coefficients are, however, little changed. Electron irradiation also affects the magnetoresistance and Hall coefficients of pyrolytic carbon as can be seen in Figs. 4 and 5. As the electron fluence increases, Hall coefficient at 30 K increases and the magnetoresistance at 30 K becomes more and more negative.

Effects of annealing up to 300 K after irradiation are presented in Fig. 6. At the low temperature region, about 25% of irradiation-induced decrease in the zero-field resistivity is

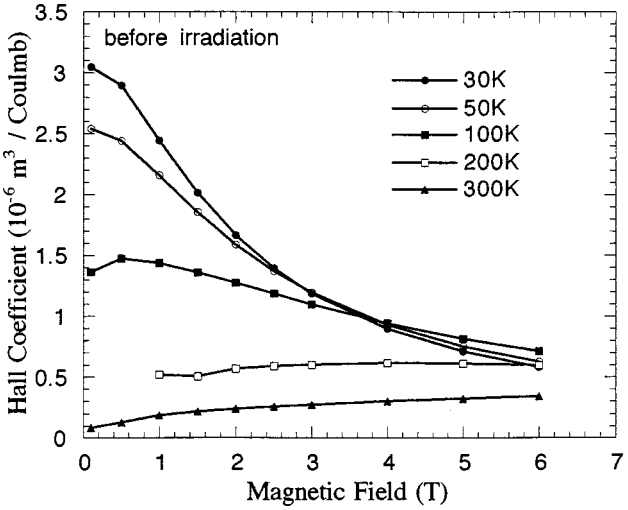

FIG. 2. Hall coefficient of unirradiated pyrolytic carbon as a function of magnetic field at various temperatures.

recovered by the annealing. The thermal annealing effect was also observed in the magnetoresistance.

IV. DATA ANALYSIS BY USING A SIMPLE TWO-BAND MODEL

A. Simple two-band model

To analyze the present result, we use a simple two-band model assuming that the hole mobility μ_h, is equal to the electron mobility μ_e. The resulting expression for the electrical resistivity under the magnetic field H, is[25,26]

$$\rho(H)=\frac{1+\mu^2H^2}{e\mu(p+n)\left[1+\mu^2H^2\left(\frac{p-n}{p+n}\right)^2\right]}, \tag{2}$$

and the Hall coefficient is[25,26]

$$R_H=\frac{(p-n)(1+\mu^2H^2)}{e[(p+n)^2+(p-n)^2\mu^2H^2]}, \tag{3}$$

where p and n are the hole and electron densities, respectively, and μ the hole and electron mobility. We assume that p and n depend on the magnetic field, and that the magnetic field does not affect the carrier mobility. The magnetoresistance can be calculated from Eqs. (1) and (2) as

$$\frac{\Delta\rho}{\rho_0}=\frac{-1+\left(\frac{p_0+n_0}{p+n}\right)\left[1+\mu^2H^2\left\{1-\frac{(p-n)^2}{(p_0+n_0)(p+n)}\right\}\right]}{1+\mu^2H^2\left(\frac{p-n}{p+n}\right)^2} \tag{4a}$$

$$=\left[-1+\left(\frac{p_0+n_0}{p+n}\right)\right]+\frac{\mu^2H^2\left(\frac{p_0+n_0}{p+n}\right)\left[1-\left(\frac{p-n}{p+n}\right)^2\right]}{1+\mu^2H^2\left(\frac{p-n}{p+n}\right)^2}, \tag{4b}$$

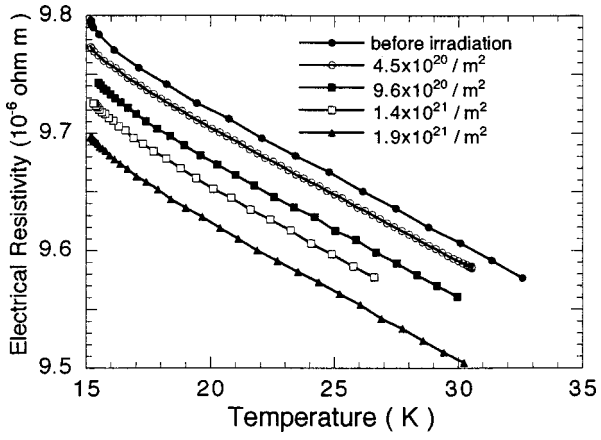

FIG. 3. Effect of electron irradiation on the zero-field electrical resistivity of pyrolytic carbon.

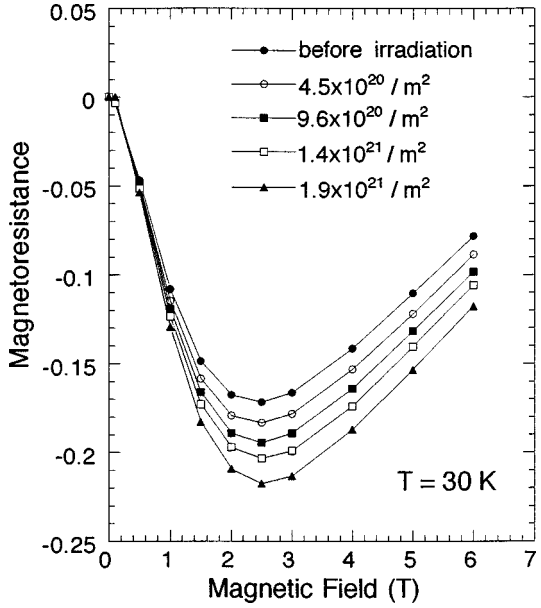

FIG. 4. Effect of electron irradiation on magnetoresistance of pyrolytic carbon. Measuring temperature is 30 K.

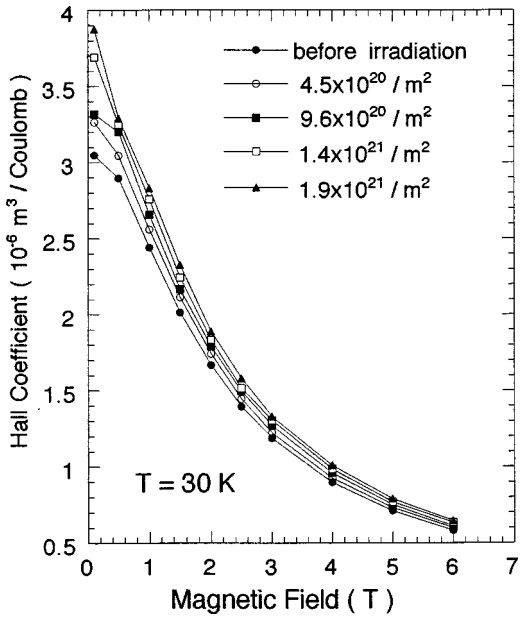

FIG. 5. Effect of electron irradiation on Hall coefficient of pyrolytic carbon. Measuring temperature is 30 K.

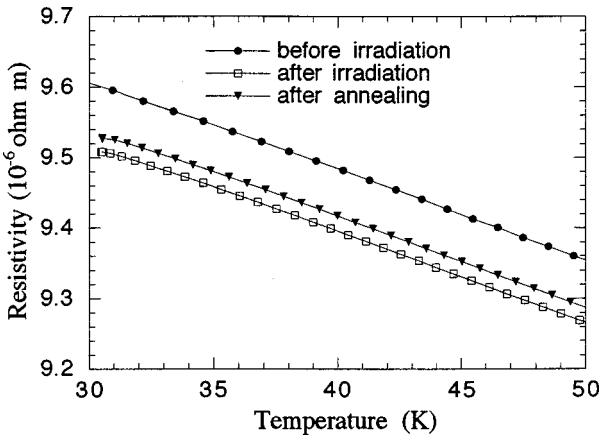

FIG. 6. Effect of thermal annealing up to 300 K on zero-field resistivity at low-temperature region.

where the subscript zero denotes the zero-magnetic-field value. The second term of the right-hand side of Eq. (4b) is always positive, while the first term becomes negative if $p+n$ increases with the magnetic field. For $p \approx n$, which is the case of well-graphitized materials, the second positive term dominates and the magnetoresistance becomes positive. For $p \gg n$ or $p \ll n$ due to the existence of acceptors or donors, respectively, the second term becomes small, and the first term dominates the magnetoresistance.

B. Electronic state of vacancy-type defects

We discuss here the electronic state of the defects in pyrolytic carbon. As we mention later, vacancy-type defects are expected to be most actively involved in the electronic properties of pyrolytic carbon.

Uemura and Inoue,[18] Yazawa,[4,19] Bright,[20] and Rahim *et al.*[11] assumed a single acceptor level for a defect state in their analyses. In neutron-irradiated graphite, it has been assumed that irradiation-produced vacancies act as electron acceptors.[27] The electronic state of these ''electron acceptors'', however, still remains unclear.

Fukuda calculated the effects of localized perturbations due to defects or impurities on the band structure of 2D graphitic material, and showed that the density of states near the Fermi energy was modified by such perturbations.[28] After that, Van Der Hoeven *et al.*[29] and Boardman, Darby, and Micah[30] showed for defect concentrations $<10^{-2}$ that the density of states differed at most by a few per cent from that of unperturbed material.

Based on these calculations, we consider the electronic state of vacancy-type defects as follows: A vacancy acts as a repulsive potential to the electrons of π bands, resulting in their deformation. The deformation appears, however, in the whole of π bands, and it does not create discrete defect levels in the π bands. As the vacancy concentration which is employed in the present study is at most ten ppm, the change in the density of states due to vacancies is negligibly small, and the rigid-band approximation can be used. The addition of single vacancies does not change the number of states of the π valence band, but decreases the number of π electrons by the number of single vacancies. In other words, the introduction of one single vacancy causes a removal of one electron from the π valence band of pyrolytic carbon. Therefore, we call such vacancy-type defects ''electron acceptor defects'', and the difference in density between hole and electron, $p-n$, is approximately related to the density of vacancies, N_V, through

$$p-n=N_V. \tag{5}$$

This relation does not depend on the temperature or magnetic field. We will use Eq. (5) later to estimate the value of carrier mobility.

Soule measured the magnetic susceptibility, electrical conductivity and Hall effect of boron-doped graphite,[31] and has found from the evaluation of the number of holes introduced by boron that ''ionization efficiency'' is about $75 \pm 15\%$. Similar to a vacancy, a boron atom that goes into the substitutional site in graphite lattice acts as a repulsive potential to π electrons. The introduction of one boron atom does not change the density of states of the π valence band of graphite, but removes one electron from the π valence band. Considering that some of boron atoms are probably trapped in imperfection sites of various types and become ineffective for the removal of π electrons, Soule's result is consistent with Eq. (5).

C. Carrier mobility

The carrier mobility, μ, is generally expressed by

$$\frac{1}{\mu}=\frac{1}{\mu_0}+\frac{1}{\mu_{irr}}=\left(\frac{1}{\mu_p}+\frac{1}{\mu_d}\right)+\frac{1}{\mu_{irr}}, \tag{6}$$

where μ_0 is the mobility for unirradiated specimen, μ_p corresponds to the scattering by phonons, μ_d the scattering by defects and/or disorder which already exist in the specimen before irradiation, and μ_{irr} the scattering by irradiation-produced defects. We estimate the value of μ for the present specimen as follows.

1. Estimate of $1/\mu_{irr}$

We consider the dependence of $1/\mu_{irr}$ on the concentration of irradiation-produced defects. As μ_{irr} is temperature independent, we use the data measured at 300 K. Figure 7(a) shows the low field ($H \leqslant 2$ T) magnetoresistance measured at 300 K before irradiation, and Fig. 7(b) shows the same measurement after the electron irradiation to $1.9\times10^{21}/\mathrm{m}^2$ at <35 K and subsequent annealing up to 300 K. Both magnetoresistances follow an H^2 dependence at 300 K. This means that the numerator of the second term of Eq. (4b) dominates the magnetoresistance, and the magnetoresistance is

$$\frac{\Delta\rho}{\rho_0}=(\mu^*)^2H^2, \tag{7a}$$

where $(\mu^*)^2$, the slope of the straight lines in Fig. 7, is given by

$$(\mu^*)^2=\mu^2\left(\frac{p_0+n_0}{p+n}\right)\left[1-\left(\frac{p-n}{p+n}\right)^2\right]. \tag{7b}$$

From Eqs. (2), (3), and (4) or (7), we can selfconsistently determine the values of the mobility, μ, at 300 K before and after irradiation as 0.201 m^2/Vs and 0.199 m^2/Vs, respec-

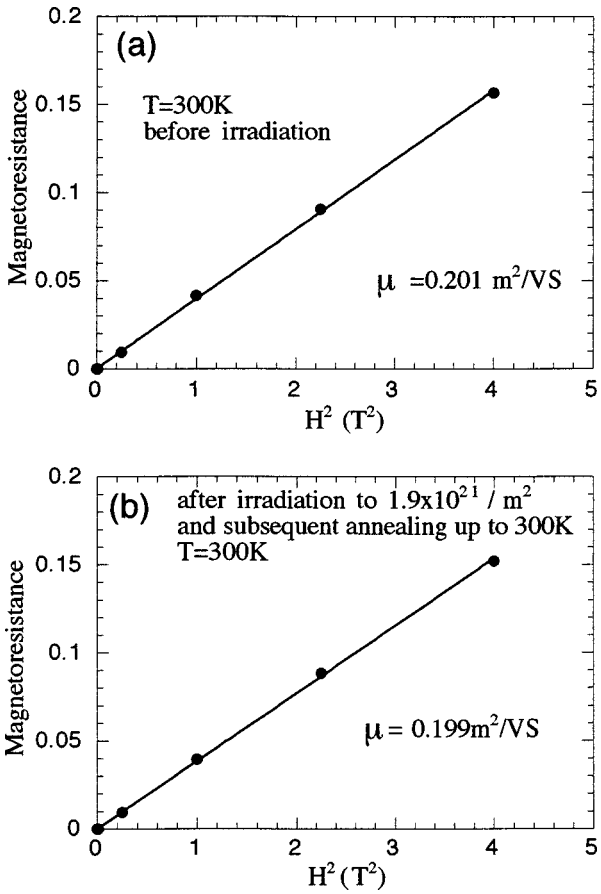

FIG. 7. H^2 dependence of room temperature magnetoresistance at low field measured (a) before irradiation, and (b) after irradiation at <35 K and subsequent annealing up to 300 K.

tively, and the difference in reciprocal mobility between before and after irradiation is 0.045 $\mathrm{Vs/m^2}$.

The reciprocal mobility after the irradiation to the fluence of $1.9\times10^{21}/\mathrm{m^2}$ was, however, measured after the subsequent annealing up to 300 K, and some parts of defects produced by irradiation had been already recovered when the magnetoresistance was measured at 300 K. From Fig. 6, we assume that about 1/4 of the irradiation-produced defects was annihilated during the annealing to 300 K. Therefore the change in the reciprocal carrier mobility at 30 K after the irradiation to the fluence of $1.9\times10^{21}/\mathrm{m^2}$ should be $0.045\times(4/3)=0.060\ \mathrm{Vs/m^2}$.

The concentration of defects produced by irradiation C_d, is given by $\sigma_d\Phi$, where σ_d is the defect production cross section and Φ is the electron fluence. The defect production cross section, σ_d, for 2-MeV electron irradiation to highly oriented pyrolytic graphite (HOPG) has been determined as $1.9\times10^{-27}\ \mathrm{m^2}$.[32] By using this cross section, we can calculate the value of C_d, and the change in $1/\mu_{irr}$ per unit concentration of irradiation-produced defects is estimated as

$$\Delta\left(\frac{1}{\mu_{irr}}\right)=1.7\times10^{-2}\ \mathrm{Vs/m^2}\ \text{per atomic ppm of defects.} \tag{8}$$

2. Estimate of $1/\mu_0$

We estimate the value of carrier mobility at 30 K for unirradiated specimen μ_0. First, from Eqs. (2) and (3), the ratio of R_H to $\rho(H)\mu$ is given by

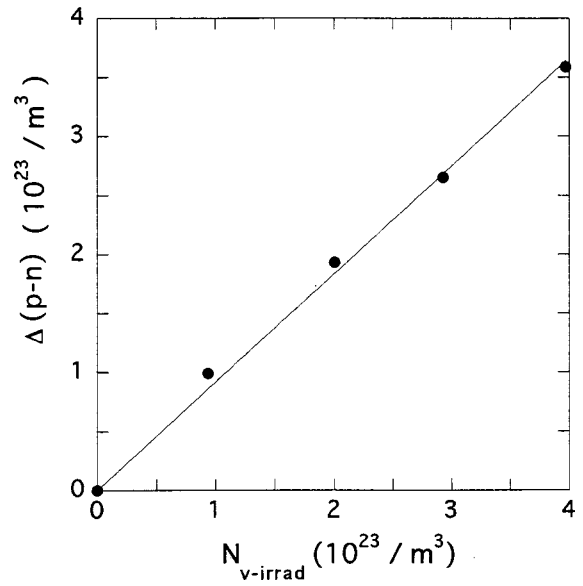

FIG. 8. Zero-magnetic field values of $\Delta(p-n)$ at 30 K as a function of $N_{\nu-\mathrm{irrad}}$ for $\mu_0=0.38\ \mathrm{m^2/Vs}$.

$$\frac{R_H}{\rho(H)\mu}=f\left(\frac{p}{n}\right)\equiv\frac{(p/n)-1}{(p/n)+1}. \tag{9}$$

As the value of $f(p/n)$ cannot exceed 1, the value of μ have to be larger than $R_H/\rho(H)$. Therefore, μ_0 should be larger than 0.36 $\mathrm{m^2/Vs}$.

Next, a clue to the estimation of μ_0 can be obtained from the relation of Eq. (5). In the following, we assume that the irradiation-produced defects which are involved in the electronic properties are vacancies, as discussed later. For electron-irradiated specimen, Eq. (5) becomes

$$p-n=N_{\nu-\mathrm{intrinsic}}+N_{\nu-\mathrm{irrad}}, \tag{10}$$

and the change in $p-n$ due to irradiation has to satisfy the relation

$$\Delta(p-n)=N_{\nu-\mathrm{irrad}}, \tag{11}$$

where $N_{\nu-\mathrm{intrinsic}}$ is the density of vacancies already-existing in the specimen before irradiation and $N_{\nu-\mathrm{irrad}}$ is that of irradiation-produced vacancies, which can be estimated as

$$N_{\nu-\mathrm{irrad}}=\Phi\sigma_d N. \tag{12}$$

Here, N is the number of carbon atoms per unit volume $[1.1\times10^{29}/\mathrm{m^3}$ (Ref. 33)].

We consider the experimental ratio of $\Delta(p-n)$ to $N_{\nu-\mathrm{irrad}}$. This ratio is called the ionization efficiency and is ideally 1.0. We calculated the ionization efficiency for an a priori assumed μ_0 from the experimental data using Eqs. (2), (3), (6), (8), and (12). The result was 0.95, 0.92, 0.87, and 0.75 for the assumed μ_0 of 0.37, 0.38, 0.40, and 0.45 $\mathrm{m^2/Vs}$, respectively. The values of μ_0 above 0.45 $\mathrm{m^2/Vs}$ give too small ionization efficiency and should be discarded.

Moreover, for μ_0 above 0.4 $\mathrm{m^2/Vs}$, $\Delta(p-n)$ becomes to show the remarkable dependence on the magnetic field. These results are inconsistent with the theoretical prediction of Eq. (11).

Considering the uncertainty in the measurements of electron fluence and the defect production cross section, we can

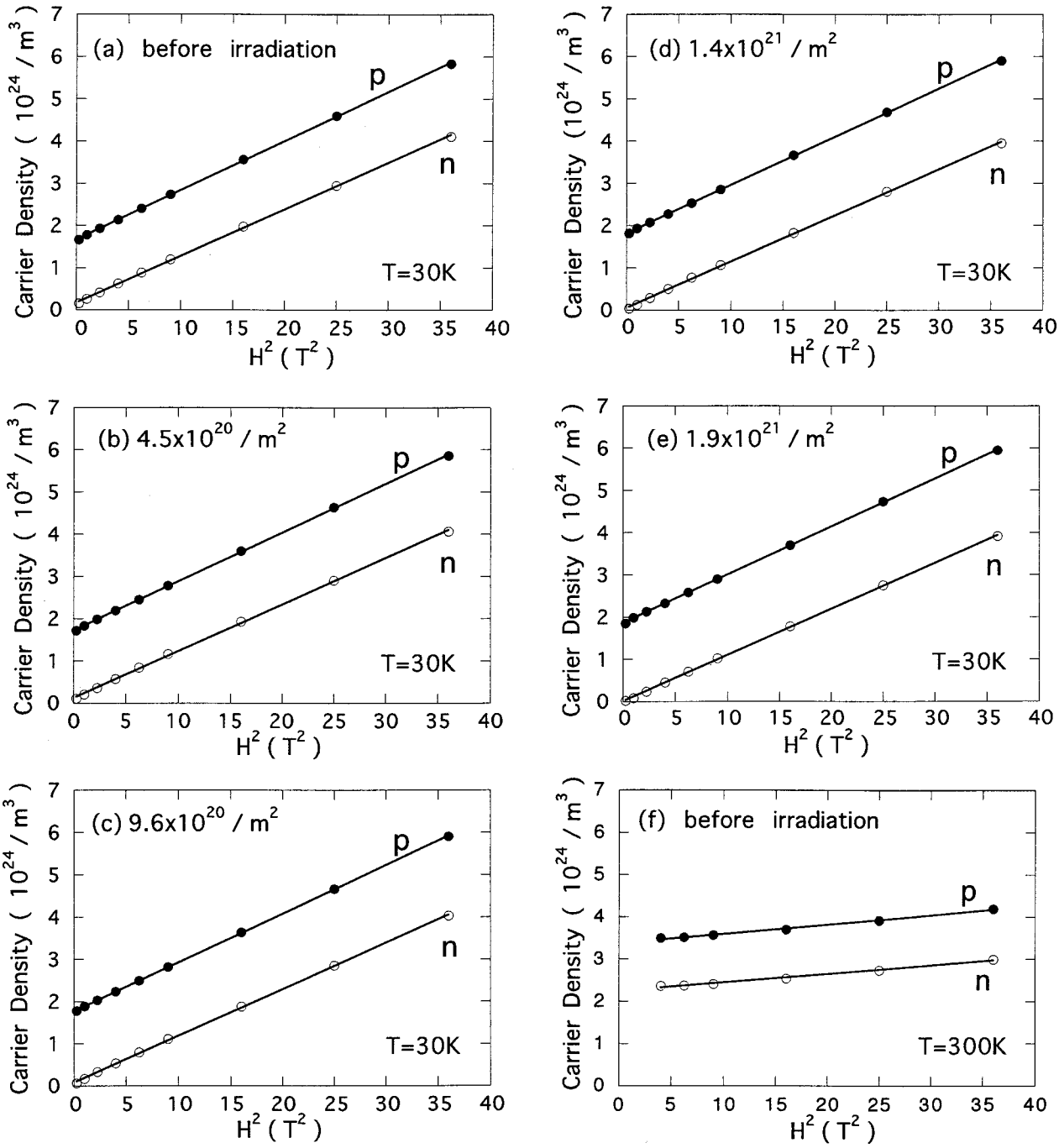

FIG. 9. Densities of holes and electrons at 30 K as a function of H^2 at various electron fluences; (a) before irradiation, (b) for $4.5\times10^{20}/\mathrm{m}^2$, (c) for $9.6\times10^{20}/\mathrm{m}^2$, (d) for $1.4\times10^{21}/\mathrm{m}^2$, and (e) for $1.9\times10^{21}/\mathrm{m}^2$. (f) shows densities of p and n at 300 K before irradiation as a function of H^2.

reasonably assume that the carrier mobility at 30 K for the unirradiated specimen is 0.38 m^2/Vs.

Thus, the carrier mobility at 30 K is given as

$$\frac{1}{\mu}=2.6+0.017c_d(\mathrm{Vs/m}^2), \tag{13}$$

where c_d is the concentration of irradiation-produced vacancies in atomic ppm. Equation (13) shows that the effect of the present irradiation on μ is quite small; μ differs at most about 1% from μ_0. Using Eq. (13), we have calculated the $N_{\nu-\mathrm{irrad}}$ dependence of $\Delta(p-n)$; the result is shown in Fig. 8. $\Delta(p-n)$ is proportional to $N_{\nu-\mathrm{irrad}}$, and the ionization efficiency is nearly 1. The uncertainty of μ affects the numerical results of p and n, but has no essential effects on the conclusion of the present paper.

D. Dependence of electron and hole densities on magnetic field and defect density

Substituting the values of the carrier mobility given by Eq. (13) into Eqs. (2) and (3), we can calculate the density of holes and electrons at 30 K as functions of magnetic field and electron fluence (or density of irradiation-produced va-

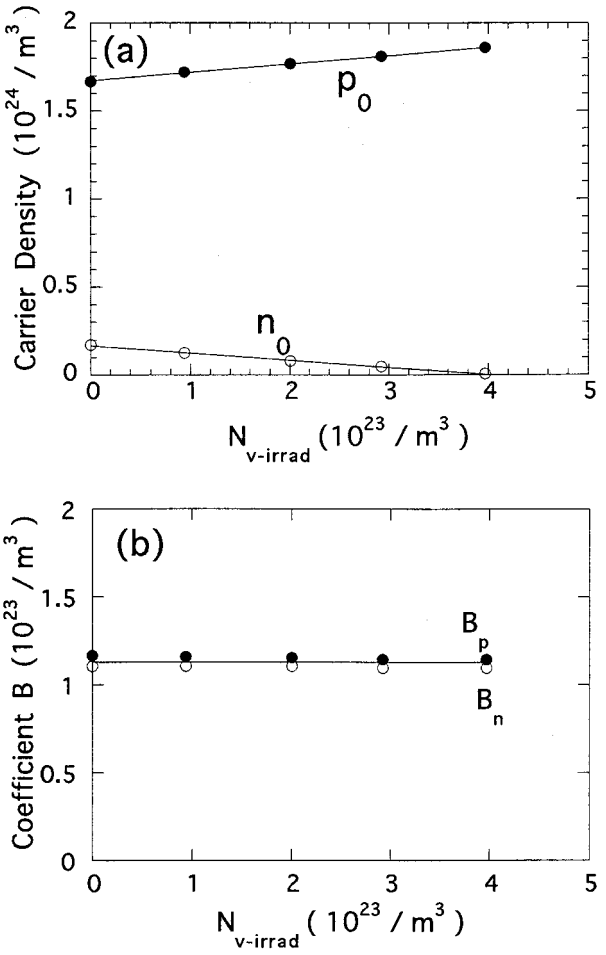

FIG. 10. (a) $N_{\nu-\mathrm{irrad}}$ dependence of p_0 and n_0. (b) $N_{\nu-\mathrm{irrad}}$ dependence of the coefficients B_p and B_n.

cancies, $N_{\nu-\mathrm{irrad}}$). The carrier densities at 300 K were also calculated for the unirradiated specimen. The result of the calculation is presented in Figs. 9(a)–9(f). As shown in the figures, the density of carriers follows the H^2 dependence at a given $N_{\nu-\mathrm{irrad}}$, and is expressed as

$$p = p_0 + B_p H^2, \tag{14a}$$

$$n = n_0 + B_n H^2, \tag{14b}$$

where p_0 and n_0 are the carrier densities for the zero-magnetic field. The dependence of p_0 and n_0 on $N_{\nu-\mathrm{irrad}}$ at 30 K is presented in Fig. 10(a). With increasing $N_{\nu-\mathrm{irrad}}$, p_0 linearly increases, while n_0 linearly decreases. Figure 10(b) shows that B_p is nearly equal to B_n at 30 K and they hardly depend on $N_{\nu-\mathrm{irrad}}$, i.e.,

$$B_p = B_n = B. \tag{15}$$

Then, Eq. (14) is reduced to

$$p = p_0 + BH^2, \tag{16a}$$

$$n = n_0 + BH^2. \tag{16b}$$

From Eq. (16), we can deduce the relation of

$$p - n = p_0 - n_0. \tag{17}$$

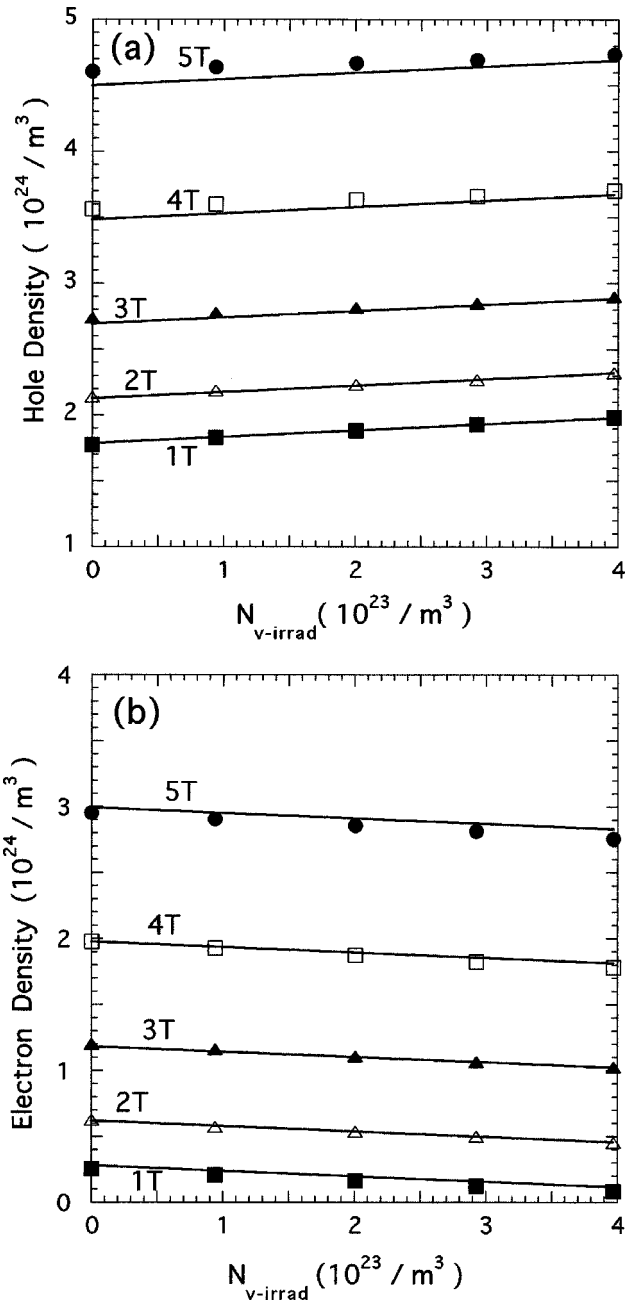

FIG. 11. (a) $N_{\nu-\mathrm{irrad}}$ dependence of hole density, p, at 30 K for various magnetic fields. Solid lines are from the calculation by Eq. (20a), (b) $N_{\nu-\mathrm{irrad}}$ dependence of electron density n, at 30 K for various magnetic fields. Solid lines are from the calculation by Eq. (20b).

Equation (17) means that the value of $p-n$ does not depend on the magnetic field. Besides, the comparison of Figs. 9(a) and 9(f) shows that $p-n$ does not depend on the temperature either. Here, we can confirm that $p-n$ depends only on the density of vacancies.

In Figs. 11(a) and 11(b), p and n are plotted against the density of irradiation-produced vacancies, $N_{\nu-\mathrm{irrad}}$, for various magnetic fields. As p increases and n decreases with $N_{\nu-\mathrm{irrad}}$, the values of p/n at a given magnetic field increase with $N_{\nu-\mathrm{irrad}}$. This $N_{\nu-\mathrm{irrad}}$ dependence of p/n is a main reason why the negative magnetoresistance is enhanced by

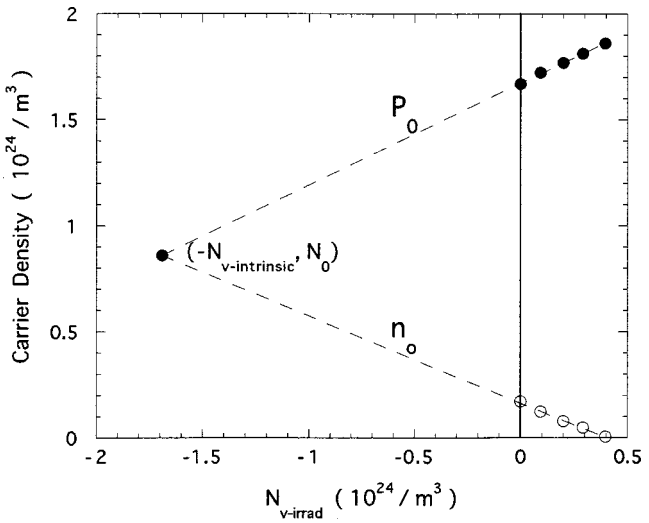

FIG. 12. Same as Fig. 10(a) except that the straight lines for p_0 and n_0 are extrapolated to their intersecting point.

electron irradiation as is proved by Eq. (4b). That is because, as $N_{\nu-\mathrm{irrad}}$ increases for a given H, $[(p-n)/(p+n)]^2$ increases with p/n, while $p+n$ hardly changes.

V. DISCUSSION

First, we consider the effect of intrinsic and irradiation-produced vacancies on the carrier densities.

The two straight lines in Fig. 10(a), which express the linear dependence of p_0 and n_0 on $N_{\nu-\mathrm{irrad}}$, intersect at a negative $N_{\nu-\mathrm{irrad}}$ value, where p_0 and n_0 have a same value of N_0 (see Fig. 12). The case $p_0=n_0$ means that there exist no acceptor defects (vacancies) in the specimen, and then the absolute value of the x axis at the intersecting point gives the density of intrinsic vacancies, $N_{\nu-\mathrm{intrinsic}}$. The value of N_0 can be considered as the additional carrier density due to the small 3D band overlap effect and the thermal excitation of carriers. The contribution of the thermal excitation can be separated if we measure N_0 as a function of temperature.

From Fig. 12, the dependence of p_0 and n_0 at 30 K on the vacancy density is given as

$$p_0=N_0+K_pN_\nu, \tag{18a}$$

$$n_0=N_0+K_nN_\nu, \tag{18b}$$

and

$$N_\nu=N_{\nu-\mathrm{intrinsic}}+N_{\nu-\mathrm{irrad}}. \tag{18c}$$

where $N_0=8.6\times10^{23}/\mathrm{m}^3$ and $N_{\nu-\mathrm{intrinsic}}=1.7\times10^{24}/\mathrm{m}^3$. The coefficient K_p is positive and K_n is negative. The value of K_p-K_n, which little depend on the temperature or the magnetic field, is nearly 1. Equation (18) means that both intrinsic and irradiation-produced vacancies act as electron acceptors, and they increase p and decrease n.

Next we discuss the effect of the magnetic field on p and n. Based on McClure's theory,[17] Bright incorporated the effects of the collision broadening of the Landau level as a result of defect and phonon scattering, and calculated the density of states, $g(E,H,\lambda^{-1})$, as a function of electron energy E, magnetic field H, and width of each Landau level, λ^{-1}.[20] If the carrier mobility and the Fermi energy are small, and the magnetic field is not so high, the resultant density of states depends only on H and λ^{-1}, and is expressed by

$$g(E,H,\lambda^{-1})\cong g(0,H,\lambda^{-1})=a+bH^2. \tag{19}$$

The coefficients, a and b, depend on λ^{-1}. If the Fermi energy does not depend on the magnetic field, the carrier densities, p and n, show the same H^2 dependence as Eq. (19). As can be seen in Fig. 9, the experimental results are in good agreement with the Bright theory. This implies that the 2D Landau levels and their broadening are realized in the specimen under the magnetic field. From Eqs. (16) and (18), the carrier densities, p and n, under the magnetic field H, are

$$p(H,N_\nu)=N_0+K_pN_\nu+BH^2 \tag{20a}$$

$$n(H,N_\nu)=N_0+K_nN_\nu+BH^2. \tag{20b}$$

Figures 11(a) and 11(b) show that the solid lines calculated using Eq. (20) can well reproduce the experimentally determined p and n.

According to the Bright theory, the coefficient B depends on the carrier mobility or the broadening of 2D Landau level. In the present experiment, however, B is nearly constant against $N_{\nu-\mathrm{irrad}}$. The carrier mobility and the broadening of the Landau level are little changed by irradiation. Electron irradiation only causes the increase in the density of vacancies which act as electron acceptors.

It should be noted that in the present analysis we have not needed to assume the existence of the discrete acceptor levels, which was a main assumption in the previous analyses.[4,11,18–20]

Finally, we discuss the effects of thermal annealing up to 300 K on the zero-magnetic field resistivity and the negative magnetoresistance. In HOPG irradiated with electrons at low temperatures, several recovery stages of resistivity have been found in the wide-temperature range.[34–38] It is known that irradiation with 1–3 MeV electrons produces single interstitials and single vacancies.[32] As single interstitial atoms in graphite can move rapidly even at low temperatures and vacancies cannot move below ~1000 °C, the recoveries of resistivity observed in HOPG below room temperature are attributed to the motion of interstitial atoms.

In the present pyrolytic carbon specimen, although the recoveries of the zero-field resistivity and the negative magnetoresistance are observed, the amount of the recovery after annealing up to 300 K is much smaller than for HOPG. Then, the reverse annealing around 100 K, which is one of the characteristics for electron and neutron-irradiated HOPG, cannot be found. This experimental result suggests that, because of a larger layer spacing and a small crystalline size, some of interstitial atoms have already migrated during irradiation at <35 K to disappear at grain boundaries and others have agglomerated to form interstitial clusters, which are not active electronically. In addition, previous stored energy release experiments on HOPG (Refs. 39 and 40) show that interstitial atoms cannot recombine with vacancies at these low temperatures. Therefore, single vacancies can survive the irradiation at <35 K and make a major contribution to the enhancement of negative magnetoresistance. The result of thermal annealing, therefore, justifies the assumption used

through this report that acceptor defects produced by irradiation are mainly single vacancies.

As the present specimen has been deposited at about 2200 °C, most of the intrinsic defects, which already exist in the specimen before irradiation, are presumably vacancy-type defects, as interstitial-type defects are unstable at high temperatures. The density of intrinsic vacancies is, however, only $1.7\times10^{24}/m^3$, as shown in Fig. 12. Therefore, even a small amount of irradiation produced vacancies ($9.4\times10^{22}-4.0\times10^{23}/m^3$) has a large effect on the electronic transport properties of pyrolytic carbon.

VI. SUMMARY

As-deposited pyrolytic carbon was irradiated with 2-MeV electrons at <35 K, and the electronic transport properties were measured at 30 K as a function of electron fluence. With increasing the electron fluence, the zero-field resistivity decreased, the Hall coefficient increased and the negative magnetoresistance became more negative.

The experimental data were analyzed by using a simple two-band model and a theoretically predicted relation of $p-n=N_\nu$. The hole and electron densities were obtained as functions of magnetic field and the density of irradiation-produced vacancies. At a given density of vacancies, the carrier densities, p and n, increase linearly with the square of the magnetic field. On the other hand, at a given magnetic field, p increases and n decreases linearly with the vacancy density. From the dependence of p and n on the magnetic field and the vacancy density, we can conclude that the negative magnetoresistance in pyrolytic carbon is attributed to the existence of acceptor defects, the two dimensionality of conduction electrons and the broadening of 2D Landau levels induced by disorder. Then, the result of electron irradiation clarifies that the vacancy-type defects, in particular single vacancies, are most actively involved in the appearance of the negative magnetoresistance in pyrolytic carbon.

ACKNOWLEDGMENTS

We are grateful to the technical staff of TIARA (Takasaki Ion Accelerators for Advanced Radiation Application) at JAERI-Takasaki for their great help.

[1] S. Mrozowski and A. Chaberski, Phys. Rev. **104**, 74 (1956).
[2] K. Takeya and K. Yazawa, J. Phys. Soc. Jpn. **19**, 138 (1964).
[3] K. Takeya, K. Yazawa, N. Okuyama, H. Akutsu, and F. Ezoe, Phys. Rev. Lett. **15**, 110 (1965).
[4] K. Yazawa, J. Phys. Soc. Jpn. **26**, 1407 (1969).
[5] Y. Hishiyama, Carbon **8**, 259 (1970).
[6] Y. Hishiyama, A. Ono, and M. Hashimoto, Jpn. J. Appl. Phys. **10**, 416 (1971).
[7] P. Delhaes, P. De Kepper, and M. Uhlrich, Philos. Mag. **29**, 1301 (1974).
[8] A. A. Bright and L. S. Singer, Carbon **17**, 59 (1979).
[9] L. D. Woolf, H. Ikezi, and Y. R. Lin-Liu, Solid State Commun. **54**, 49 (1985).
[10] Y. Koike, S. Morita, T. Nakanomyo, and T. Fukase, J. Phys. Soc. Jpn. **54**, 713 (1985).
[11] I. Rahim, K. Sugihara, M. S. Dresselhaus, and J. Heremans, Carbon **24**, 663 (1986).
[12] V. Bayot, L. Piraux, J.-P. Michenaud, and J.-P. Issi, Phys. Rev. B **40**, 3514 (1989).
[13] V. Bayot, L. Piraux, J.-P. Michenaud, J.-P. Issi, M. Lelaurain, and A. Moore, Phys. Rev. B **41**, 11 770 (1990).
[14] C. A. Klein, Rev. Mod. Phys. **34**, 56 (1962).
[15] C. A. Klein, J. Appl. Phys. **35**, 2947 (1964).
[16] P. R. Wallace, Phys. Rev. **71**, 622 (1947).
[17] J. W. McClure, Phys. Rev. **104**, 666 (1956).
[18] Y. Uemura and M. Inoue, J. Phys. Soc. Jpn. **13**, 382 (1958).
[19] K. Yazawa, J. Chim. Phys. **64**, 961 (1967).
[20] A. A. Bright, Phys. Rev. B **20**, 5142 (1979).
[21] E. Abrahams, P. W. Anderson, D. C. Licciardello, and T. V. Ramakrishnan, Phys. Rev. Lett. **42**, 673 (1979).
[22] L. Piraux, V. Bayot, X. Gonze, J.-P. Michenaud, and J.-P. Issi, Phys. Rev. B **36**, 9045 (1987).
[23] L. Piraux, V. Bayot, J.-P. Issi, M. S. Dresselhaus, M. Endo, and T. Nakajima, Phys. Rev. B **41**, 4961 (1990).
[24] G. Bergmann, Phys. Rep. **107**, 1 (1984).
[25] J. M. Ziman, *Principles of the Theory of Solids* (Cambridge University Press, London, 1972), Chap. 7.
[26] P. Delhaes, in *Chemistry and Physics of Carbon*, edited by P. L. Walker, Jr. (Dekker, New York, 1971), Vol. 7, pp. 193–235.
[27] B. T. Kelly, *Physics of Graphite* (Applied Science Publishers, London, 1981), Chap. 7.
[28] Y. Fukuda, J. Phys. Soc. Jpn. **20**, 353 (1965).
[29] B. J. C. Van Der Hoeven, Jr., P. H. Keesom, J. W. McClure, and G. Wagoner, Phys. Rev. **152**, 796 (1966).
[30] A. D. Boardman, M. I. Darby, and E. T. Micah, Carbon **11**, 207 (1973).
[31] D. E. Soule, *Proceedings of the Fifth Conference on Carbon* (Pergamon, New York, 1962), Vol. 1, p. 13.
[32] T. Iwata and T. Nihira, J. Phys. Soc. Jpn. **31**, 1761 (1971).
[33] C. A. Klein, J. Appl. Phys. **33**, 3338 (1962).
[34] S. B. Austerman and J. E. Hove, Phys. Rev. **100**, 1214 (1955).
[35] T. Iwata, T. Nihira, and H. Matsuo, J. Phys. Soc. Jpn. **33**, 1060 (1972).
[36] W. N. Reynolds and P. R. Goggin, Philos. Mag. **5**, 1049 (1960).
[37] T. Iwata, T. Nihira, and T. Ohmichi, Carbon **6**, 742 (1968).
[38] T. Iwata, T. Nihira, and H. Matsuo, J. Phys. Soc. Jpn. **36**, 123 (1974).
[39] T. Iwata and T. Nihira, Jpn. J. Appl. Phys. **15**, 575 (1976).
[40] L. Bochirol and E. Bonjour, Carbon **6**, 661 (1968).